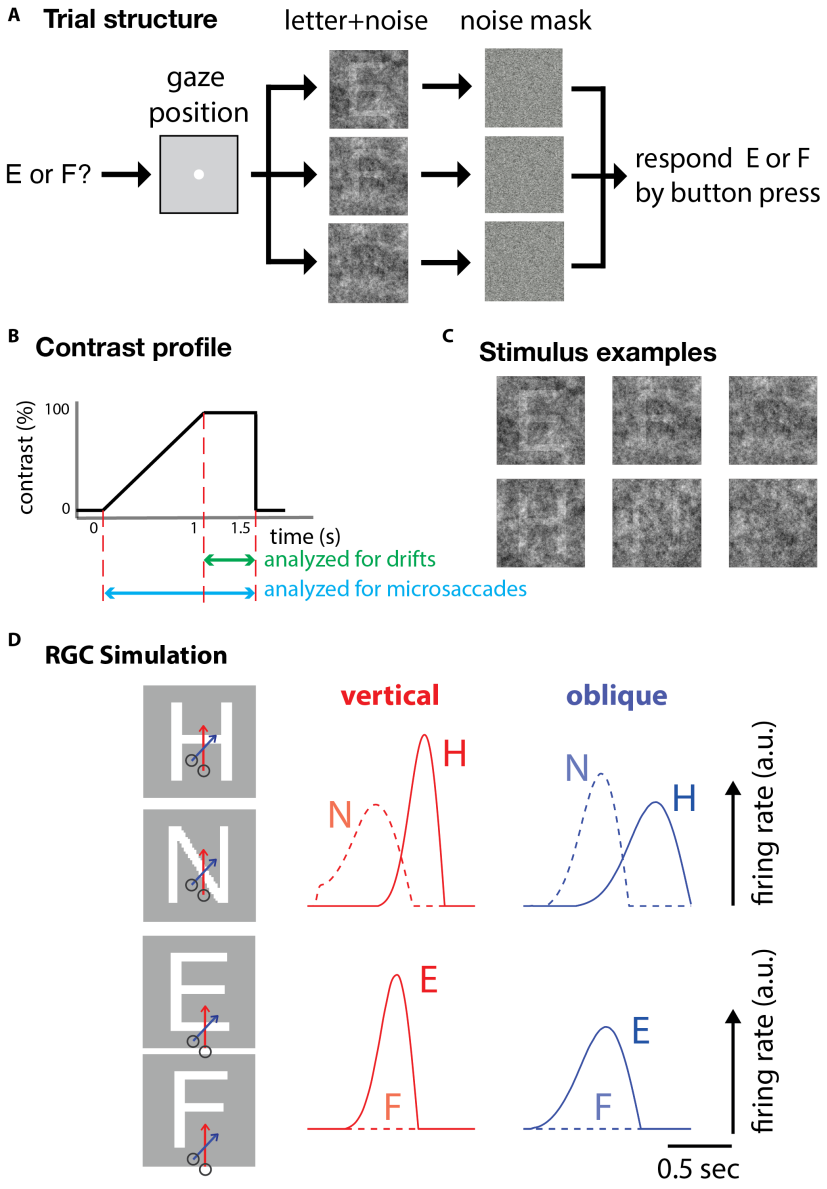

Figure S1: Task structure and model RCG responses, Related to STAR Methods and Figure 1 (A) The trial structure of the letter discrimination task. (B) The contrast ramp used in each trial. (C) Stimulus examples. Top row shows E, F, and letter-absent; bottom row shows H, N, and letter-absent. (D) Simulated firing profiles of an RGC moving across the letters. The size of the modeled receptive field center is indicated by the circle at the beginning of each trajectory; surround radius is four times larger. Eye motion was simulated as as vertical movement (moving from bottom to the top) or oblique movement (moving from lower left to upper right) at a constant speed at 0.5 deg/sec for 0.8 sec.

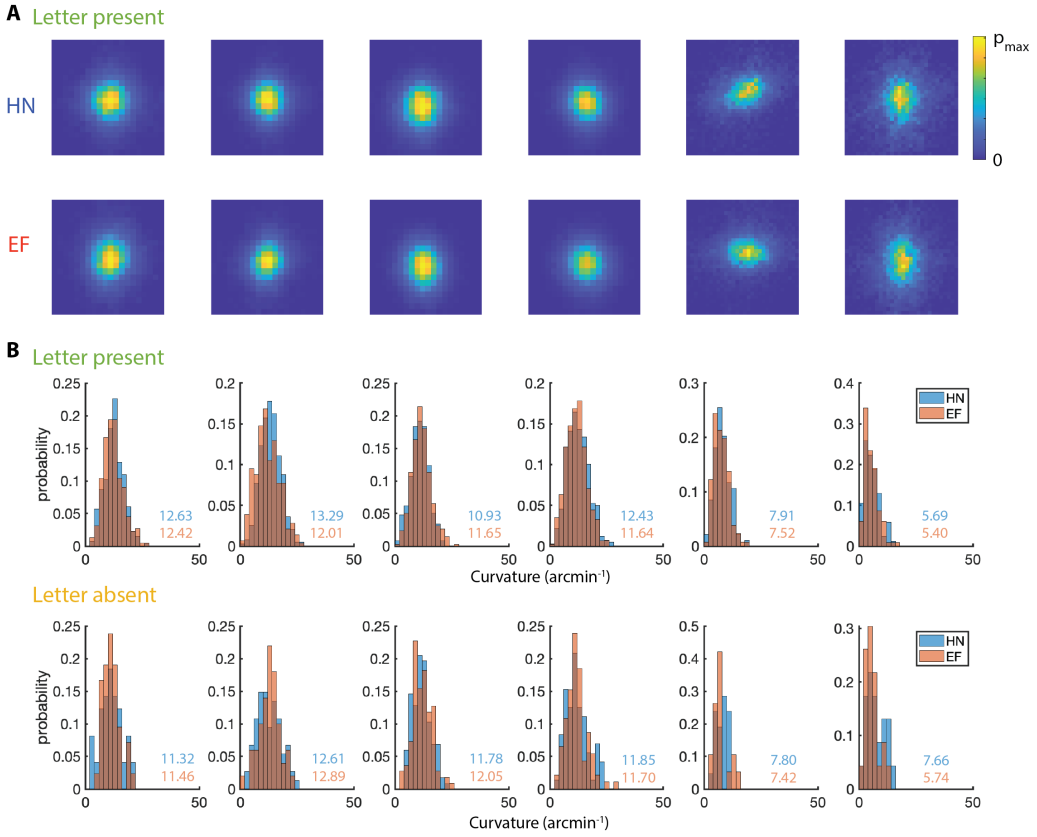

Figure S2: Drift velocity heatmap, drift orientations, and curvatures, Related to Figure 2 (A) Drift velocity distribution of each subject (S1-6 from left to right) from HN trials (top) and EF trials (bottom), with letter-present. Region shown is 2° per second square for S1 to S4 and 3° per second square for S5 and S6. Color bar maximum (p_{max}) is 0.0366 for S1 to S4, 0.0163 for S5, and 0.0121 for S6. (B) Histograms of mean curvatures of each trial from HN trials and EF trials, with letter-present (top) and letter-absent (bottom). There was no difference in the distribution of curvature values for HN vs. EF conditions within any subject (two-tailed Wilcoxon signed rank test, $p > 0.05$ for each subject individually), and there was no difference in mean curvature values between the two trial types across subjects (two-tailed paired t-test, $p > 0.05$). Numbers in each subpanel indicate mean curvature for each condition, in arcmin^{-1}.

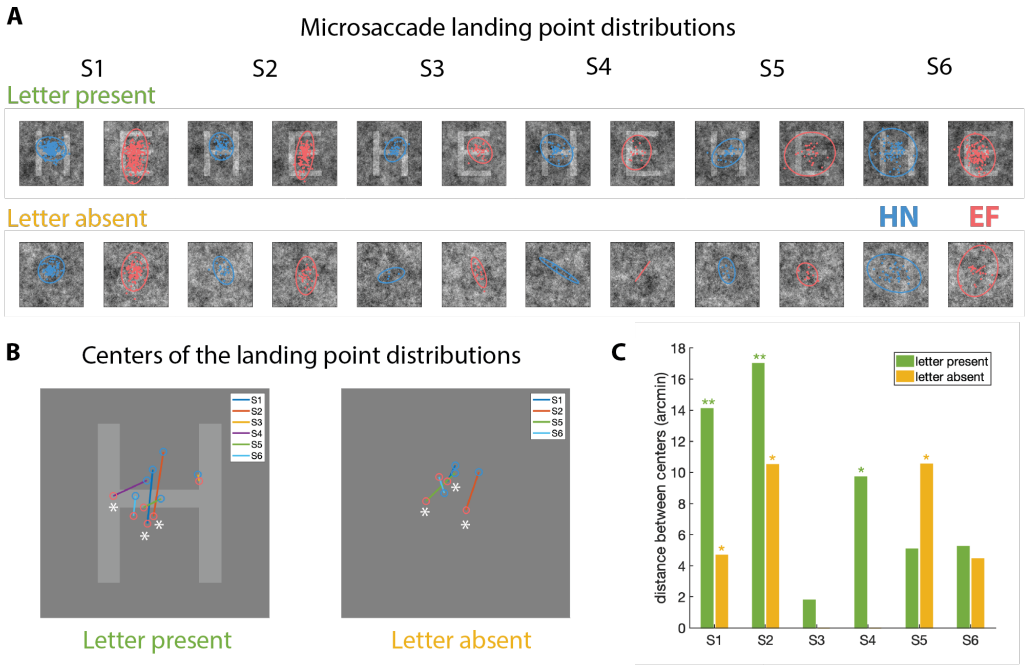

Figure S3: Comparison of microsaccade landing points between HN and EF blocks, Related to Figure 2 (A) Microsaccade landing points on each target, along with minimum-area ellipses covering 95% of the landing points. (B) Centers of landing point ellipses in HN trials (blue circles) and EF trials (red circles). * labels the statistically-significant differences (see panel C for significance level).(C) Euclidean distances between the centers of HN and EF distributions. Green: letter-present trials. Orange: letter-absent trials. Null distributions obtained by shuffling and significant difference are represented by * as $p<0.05$ and ** as $p<0.01$. No data are shown for letter-absent trials of subjects 3 & 4 because of the low number of microsaccades (see Table S1). Similar results were observed for microsaccade starting positions.

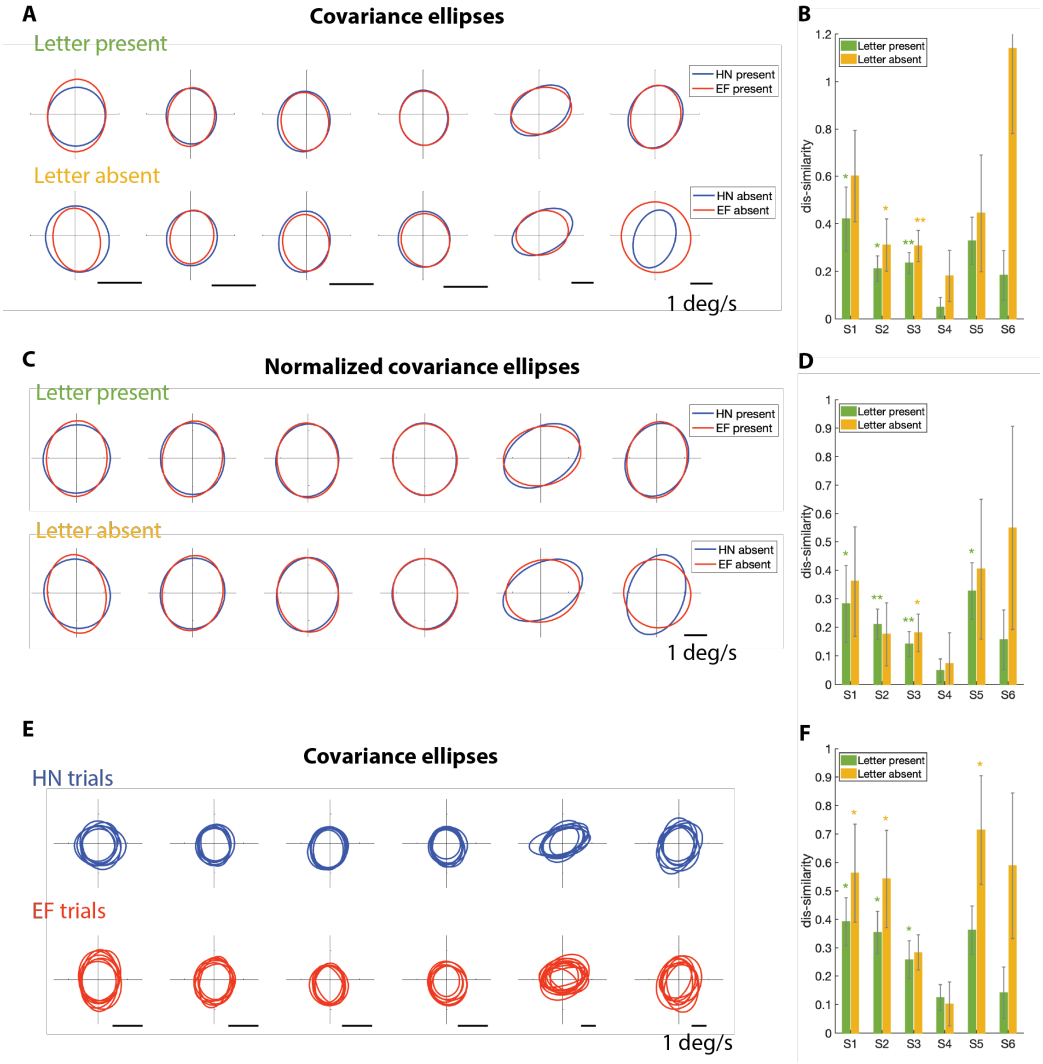

Figure S4: Additional drift analysis and statistics, Related to Figure 2 (A-D) Drift velocity statistics with 100-ms holdout from non-drift eye movements (A) Top: Drift velocity covariance ellipses from trials in HN block (blue) and EF block (red) superimposed. Bottom: Same as top panel but from letter-absent trials. (B) Dis-similarity between HN and EF covariance ellipses from six subjects. Green: letter-present trials. Orange: letter-absent trials. (Error bars: 1 standard deviation. * $p<0.05$, ** $p<0.01$) (C & D) The same analysis applied to covariance ellipses after normalizing to the same total area. **(E-F) Balanced block shuffling** (E) Drift velocity covariance ellipses from each block. (F) Dis-similarity statistics between HN and EF covariance ellipses from six subjects.

Data type	Letter	Stimulus	S1	S2	S3	S4	S5	S6
trials	HN	present	451	433	360	377	142	172
		blank	127	115	110	72	42	37
	EF	present	443	416	412	342	172	114
		blank	99	103	107	66	37	32
drift segments	HN	present	265	379	352	418	91	81
		blank	47	67	116	71	20	21
	EF	present	198	242	407	419	125	111
		blank	40	36	110	88	16	19
microsaccades	HN	present	170	55	36	38	30	67
		blank	80	16	4	4	8	30
	EF	present	232	125	28	12	102	26
		blank	85	32	11	3	21	11

Table S1: Summary of the numbers of trials given conditions in all six subjects, Related to STAR Methods Number of trials, drift segments, and microsaccdes free from artifacts.